Tailoring the Architecture of Cationic Polymer Brush Modified Carbon Nanotubes for Efficient siRNA Delivery in Cancer Immunotherapy

*Danyang Li[1], Momina-Ahmed[1], Anisah Khan[1], Lizhou Xu[1], Adam A Walters[1], Belén Ballesteros[2], Khuloud T. Al-Jamal[1]**

[1]Institute of Pharmaceutical Science, Faculty of Life Science & Medicine, King's College London, Franklin-Wilkins Building, 150 Stamford Street, London, SE1 9NH UK
[2]Catalan Institute of Nanoscience and Nanotechnology (ICN2), CSIC and BIST, Campus UAB, Bellaterra, 08193 Barcelona, Spain

*Corresponding author:

khuloud.al-jamal@kcl.ac.uk

Keywords: carbon nanotubes, cationic polymer brush, polydopamine chemistry, atom transfer radical polymerisation, nucleic acids interaction, siRNA delivery

Table of Content

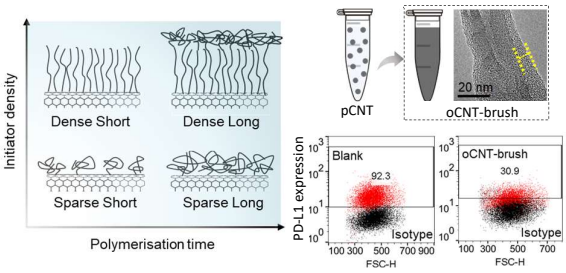

Abstract

Facile and controlled fabrication of homogenously grafted cationic polymers on carbon nanotubes (CNTs) remains poorly investigated, which further hinders the understanding of interactions between functionalised CNTs with different nucleic acids and the rational design of appropriate gene delivery vehicles. Herein, we describe the controlled grafting of cationic poly(2-dimethylaminoethylmethacrylate) (PDMAEMA) brushes on CNTs *via* surface-initiated atom transfer radical polymerisation (SI-ATRP) integrated with mussel-inspired polydopamine (PDA) chemistry. The binding of nucleic acids with different brush-CNT hybrids discloses the highly architectural dependent behaviour with dense short brush coated CNTs displaying the highest binding among all the other hybrids, namely, dense long, sparse long and sparse short brush-CNTs. Additionally, different chemistries of the brush coatings were shown to influence the biocompatibility, cellular uptake and silencing efficiency *in vitro*. This platform provides great flexibility for the design of polymer brush-CNT hybrids with precise control over their structure-activity relationship for rational design of nucleic acids delivery systems.

Introduction

Efforts to improve synthetic gene delivery have led to the development of various delivery systems including liposomes[1-2], emulsions[3], polymeric micelles[4], hybrid nanoparticles[5], *etc*. Carbon nanotubes (CNTs) possess unique features such as the hollow structure, high aspect ratios, and other physicochemical properties which make them attractive candidates[6-7]. The applications of as-prepared CNTs as delivery systems are often limited due to persisting issues of the poor dispersibility in aqueous solutions and potential toxicity. Various surface functionalisation strategies of both covalent and non-covalent have been recently thoroughly reviewed[8]. Indeed, the role played by the surface functionalisation of CNTs is crucial and will result in different surface properties such as charge density, hydrophobicity/hydrophilicity, dispersity, chemical reactivity *etc.*, driving different interactions of CNTs with the physiological environment.

For gene delivery systems, one of the most commonly used surface functionalisation strategies is to render carbon nanotubes positively charged, thus to condense negatively charged nucleic acids. For instance, aminated tetraethylene glycol modified CNTs were shown to be able to associate plasmid DNA, resulting in 5–10 times higher levels of gene expression compared to naked plasmid.[9] The surface area and charge density of CNTs were shown to be critical for interacting with plasmid DNA and the consequent formation of a biologically active complex.[10] The development of cationic polymer and dendrimer grafted CNTs has been used to improve the dispersity, biocompatibility and transfection efficiency of CNTs. Dendrimers containing large numbers of surface primary amine groups can effectively improve the dispersion of CNTs in aqueous solution and achieve higher transfection efficiency.[11] However, the properties of dendrimers are mainly dependent on the number of their generations and the synthesis is usually complicated. Studies have shown linear polyamidoamine functionalised CNTs possessed comparable level of transfection with free polyamidoamine, but significantly lower

cytotoxicity.[12] However, CNT-assisted delivery of siRNA is still hampered by limitations in nucleic acid loading capacity and transfection efficiency. Covalent attachment of siRNA to CNTs was reported to have limited loading amount of siRNA and also the technique relies on the modifications of siRNAs which may impact potency.[13-14] Other cationic polymer e.g. poly(ethylenimine) functionalised CNTs exhibited relatively low efficiency in delivery of siRNA.[15]

Cationic polymer brushes synthesised *via* surface-initiated atom transfer radical polymerisation (SI-ATRP) are of great interest as efficient siRNA delivery systems as they offer flexibility for tailoring the surface chemistries and architectures.[16-19] Properties such as chain length, density, charge and topology of the coatings can be easily tuned and adapted to suit various applications by changing the type of monomers, initiators, ligands or the polymerisation conditions.[17, 19] Previous studies have shown dense cationic polymer brushes e.g. poly(2-dimethylaminoethylmethacrylate) PDMAEMA brushes, were able to capture siRNA stably *via* local desorption/re-adsorption and entropic stabilisation.[17] However, there is still lack of deep investigation of the interactions between nucleic acids with this dense cationic crowding. Moreover, taking advantage of the distinctive properties of CNTs, grafting cationic polymer brush on the surface provides the possibility of achieving more densely packed polymer chains compared to spherical particles, as ATRP initiator density is considered to be higher on cylindrical surfaces.[20]

Herein, cationic polymer brush grafted CNT hybrids with different chemistries and architectures were prepared utilising unique characteristics of both CNTs and polymer brushes for understanding the interactions of different nucleic acids with these brush-CNT hybrids, to be eventually applied to design efficient siRNA delivery vectors. For this purpose, we functionalised the CNTs with PDMAEMA brushes *via* mussel-inspired polydopamine (PDA) chemistry and SI-ATRP. By changing the density of the bromo initiator moieties and

polymerisation period, the density and length of the polymer chains were precisely controlled. Thus, four different types of cationic polymer brush coatings were easily synthesised on CNTs, namely, sparse short (SS), sparse long (SL), dense short (DS) and dense long (DL) PDMAEMA brush coatings. The physicochemical properties of brush-CNT hybrids were thoroughly characterised by different techniques. The binding affinity of different nucleic acids including siRNA, ssDNA and plasmid was then investigated, providing strong evidence of the architectural influence of the brush coatings on nucleic acids binding efficiency. The optimal brush-CNT hybrids were applied as carriers for the delivery of siRNA targeting program death ligand 1 (PD-L1). Finally, we have also compared the impact of different chemistries of the brush coatings which have the same architecture on the corresponding cellular response.

2. Experimental section

2.1 Materials

Pristine multi-walled carbon nanotubes (pCNTs, outer diameter = 20-30 nm, length = 0.5-2 μm, purity >95%) were purchased from Nanostructured & Amorphous Materials Inc., USA. Sulfuric acid (H_2SO_4, 98%) was purchased from Honywell Fluka^{TM}, Germany. Nitric acid (HNO_3, 65%) was purchased from Acros Organics, USA. Dopamine hydrochloride (98%), triethylamine (Et_3N, 99%), α-bromoisobutyrylbromide (α-BiBB, 98%), 2-dimethylaminoethylmethacrylate (DMAEMA, 98%), 2,2'-bipyridyl (bipy, 99%), copper (II) bromide ($CuBr_2$, 99%), copper (I) chloride (CuCl, 99.995%), iodomethane (CH_3I, 99.5%), ethanol (EtOH, >99.8%), N, N-dimethylformamide (DMF, >95%) and sodium azide were purchased from Sigma-Aldrich. Propionyl bromide (>98%) was purchased from Fluorochem Ltd. All chemicals and solvents were of analytical grades and used as received unless otherwise stated. Dopamine hydrochloride and CuCl were kept sealed until use and purged with N_2 gas after every use to avoid oxidation when exposed to air. Tris-HCl buffer (10 mM, pH 8.5) was

made from tris(hydroxymethyl)aminomethane (tris base, 99.5%) purchased from Formedium and hydrochloric acid (HCl, 37%) purchased from Sigma Aldrich. Sodium-borate-buffers (SB, pH-8) was made from sodium hydroxide (0.4 g, >98%) purchased from Honeywell FlukaTM and boric acid (2.25 g, ≥98%) purchased from Santa Cruz Biotechnology Inc. USA, dissolved in 1 L deionised water (DI H_2O, resistivity 18.2 $M\Omega^{-cm}$) obtained through PURELAB ultrapure water system. Gel loading dye purple (6X, no SDS) was purchased from New England Biolabs and mixed in equal ratio with GelRed® (6X in nuclease free water) purchased from Biotium. Invitrogen^{TM} Ultrapure^{TM} Agarose, RPMI-1640 medium, pen-strep, glutamine, fetal calf serum (FCS), trypsin, 10 X phosphate buffered saline (PBS) were purchased from ThermoFisher Scientific. Noncoding siRNA (siNEG) (anti-sense sequence, 5′-CAUCGUCGAUCGUAGCGCAA-3′), Atto 655 siNEG (Seq: UGCGCUACGAUCGACGAUG55), siPD-L1 (Seq: GAGGUAAUCUGGACAAACA), ssDNA (Seq: TCCATGAGCTTCCTGATGCT) were purchased from Eurogentec. OX40 plasmids were purchased from Stratech. Phycoerythrin (PE) anti-PD-L1 and its corresponding isotype were purchased from Biolegend.

2.2 Synthesis of cationic polymer brush coated carbon nanotubes

Cationic polymer brush coated CNTs were synthesised *via* SI-ATRP from bromo initiator moieties using a 'grafting from' approach. The reaction route is shown in Scheme 1. Four different types of hybrids, namely SS, SL, DS and DL brush coated CNTs with varied polymer chain length and density, were synthesised by changing the initiator density and polymerisation time, as shown in Scheme 2.

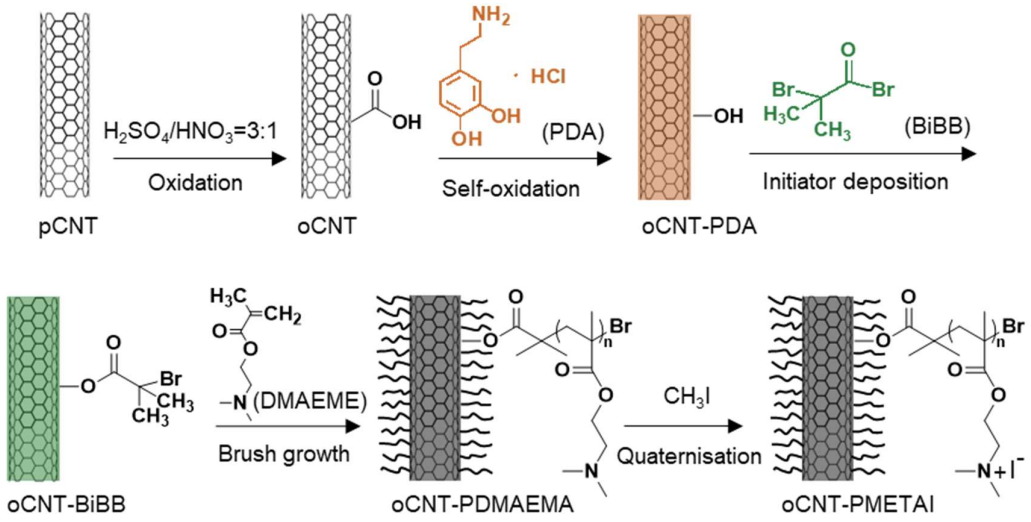

Scheme 1. Synthesis of cationic polymer brush grafted carbon nanotubes.

2.2.1 Oxidation of pristine carbon nanotubes (oCNT)

Oxidation of pristine carbon nanotubes (pCNTs) was performed adapting protocols from literature to purify, shorten and functionalise the pCNTs.[21] Briefly, a mixed acid solution of H_2SO_4 and HNO_3 with a volume ratio of 3 was prepared by adding 45 mL of H_2SO_4 into 15 mL of HNO_3 dropwise with stirring in an ice bath. 200 mg of pCNTs (20-30 nm in width) was weighed in a 250 mL round bottle flask. The mixed acid solution was added to the pCNTs under stirring by a dropping funnel at room temperature (RT). The reaction was kept stirring at RT for 3 h and then sonicated for another 3 h, after which, the reaction was kept stirring at RT overnight. The reaction was stopped by slowly pouring into 400 mL of DI H_2O whilst stirring and the products were subsequently purified through a 0.1 μm hydrophilic PC membrane filter. The oxidised carbon nanotubes (oCNTs) were collected, washed three times with DI H_2O to get rid of residual acid and finally re-dispersed in 20 mL of DI H_2O and stored in the fridge.

2.2.2 Polydopamine coating of oxidised carbon nanotubes (oCNT-PDA)

Polydopamine (PDA) was coated on oCNTs through π-π interaction with spontaneous oxidative polymerisation of dopamine hydrochloride according to a previous protocol[22-23] . oCNT dispersion (1 mg/mL, 100 mg) and dopamine hydrochloride solution (0.1 mg/mL) were prepared in 100 mL of 10 mM tris-HCl buffer (pH 8.5). The reaction mixture was kept stirring for 24 h, at RT, after which it was purified by filtering through a 0.1 μm hydrophilic PC membrane filter. The polydopamine functionalised carbon nanotubes (oCNT-PDA) were collected, washed three times with DI H_2O and finally re-dispersed in 10 mL of DI H_2O and stored in the fridge.

2.2.3 ATRP initiator deposition on oCNT-PDA (oCNT-BiBB)

ATRP initiator was anchored onto oCNT-PDA adapting protocols from literature[17, 22]. The dispersion solvent for oCNT-PDA (DI H_2O) was substituted with DMF by centrifugation at 10,000 rpm for 30 min and subsequent re-dispersion multiple times. A final concentration of oCNT-PDA in DMF of 1 mg/mL was obtained. The mixture was then divided into 2 halves. Depending on the targeted grafting density (100% or 10%), they were either coated with 100% ATRP initiator or with a mixture of ATRP initiator diluted with its non-reactive analogue at a ratio of 1:9.

2.2.3.1 Dense initiator coating (oCNT-BiBB-D)

oCNT-PDA (100 mg) was firstly dispersed in 100 mL of DMF, under N_2 protection at RT. Then 5 mL of Et_3N was added dropwise whilst stirring followed by 4.5 mL of α-BiBB initiator added dropwise whilst stirring. The reaction was left to stir overnight at RT and then the mixture was diluted with 200 mL of EtOH. Afterwards, it was purified *via* centrifugation (10,000 rpm, 30 min). The dense ATRP initiator coated carbon nanotubes (oCNT-BiBB-D) were collected and washed three times with EtOH centrifugation-sonication cycles and finally dispersed in 10 mL mixture of DI H_2O and EtOH (v/v 4:1) and stored in the fridge.

2.2.3.2 Sparse initiator coating (oCNT-BiBB-S)

This was done in the same way as the dense initiator coating except 0.45 mL of α-BiBB initiator (10% molar ratio) was mixed with 2.95 mL of propionyl bromide (non-reactive analogue, 90% molar ratio) before dropwise addition to the reaction under N_2 protection. The sparse ATRP initiator coated carbon nanotubes (oCNT-BiBB-S) were finally dispersed in 10 mL mixture of DI H_2O and EtOH (v/v 4:1) and stored in the fridge.

2.2.4 PDMAEMA brush growth on oCNT-BiBB (oCNT-PDMAEMA)

For the formation of each hybrid, a monomer solution was prepared according to our previous work[17] by dissolving the DMAEMA (13.2 g, 42 mmol), bipiridyl (640 mg, 2.05 mmol) and $CuBr_2$ (36 mg, 80 mmol) in 30 mL of DI H_2O and EtOH (v/v 4:1) mixed solvent and degassed with N_2 whilst stirring for 30 min. Then CuCl (168 mg, 0.828 mmol) was added quickly to this solution and it was further degassed with N_2 whilst stirring for 5 min. oCNT-BiBB-D and oCNT-BiBB-S with 5 mg/mL in DI H_2O and EtOH (v/v 4:1) mixed solvent were also degassed with N_2 purging whilst stirring for 30 min. An equal volume of monomer solution was injected under inert atmosphere *via* a syringe to each of the oCNT-BiBB batches and polymerisation was allowed to proceed under N_2 at RT. For the short brush, polymerisation was terminated at 15 min, whereas for the long brush, it was terminated at 240 min. Hereby, the four types of PDMAEMA brush coated carbon nanotube hybrids (oCNT-PDMAEMA) were formed, named as oCNT-SS for SS PDMAEMA brush-CNT hybrids, oCNT-SL for SL brush coatings, oCNT-DS for DS coatings and oCNT-DL for DL coatings, respectively (Scheme 2). Polymerisation was terminated by immediate exposure to atmosphere and immersion of each sample in 100 mL of DI H_2O followed by bubbling with air whilst stirring until a colour change from dark brown to blue was observed (oxidation of CuCl). The four different types of polymer brush coated CNTs were collected *via* centrifugation (10,000 rpm, 30 min) and each was washed with DI H_2O and EtOH successively in centrifugation-sonication cycles until the filtrate turned

clear to get rid of the residual monomer, ligand and catalysts. oCNT-PDMAEMA was finally dispersed in 10 mL of DI H_2O each and stored in the fridge.

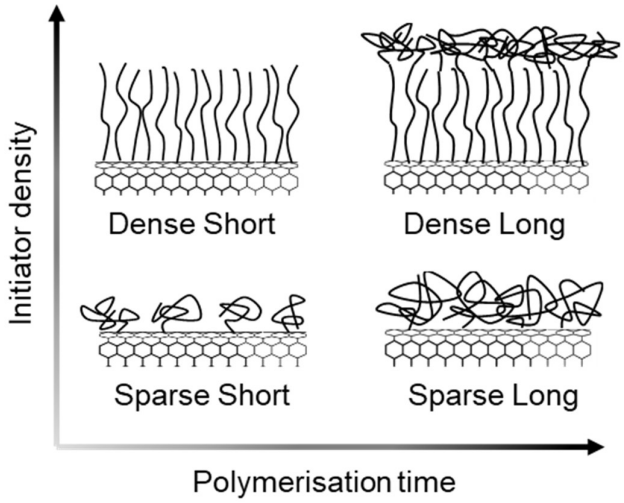

Scheme 2. **Schematic illustration of different architectures of cationic polymer brush grafted carbon nanotubes.** Different brush-CNT hybrids were prepared by precious control over polymerisation conditions and the deposition of initiators with different densities.

2.2.5 Synthesis of oCNT-PMETAI

The tertiary amines of PDMAEMA brushes on CNT were quaternised by methyl iodide to obtain poly{[2-(methacryloyloxy)ethyl] trimethylammonium iodide} (PMETAI) brushes coated CNTs (oCNT-PMETAI). First, the dispersion solvent for each type of oCNT-PDMAEMA (DI H_2O, 50 mg) was replaced with 10 mL of DMF by centrifugation and subsequent redispersion. Then 0.1 mL of CH_3I was added to each reaction and left to stir in the dark for 24 h, at RT. Afterwards, the reactions were purified by centrifugation (10,000 rpm, 20 min) and the product was washed with DI H_2O in centrifugation-sonication cycles for three times and finally re-dispersed in 5 mL of DI H_2O and stored in the fridge. Each brush-CNT hybrid was named as oCNT-SSI+, oCNT-SLI+, oCNT-DSI+ and oCNT-DLI+, respectively, after quaternisation.

2.3 Physicochemical characterisation of cationic polymer brush coated carbon nanotubes

Each step of the synthesis was monitored using various qualitative and quantitative techniques to ascertain the correct functionalisation had occurred.

2.3.1 Dispersion quality

The dispersibility of the CNTs in a polar solvent and resulting stability of said colloidal suspensions were examined for pCNTs after each functionalisation step. Samples of 1 mg/mL were dispersed in 1 X PBS at RT and sonicated for 10 min and finally left to settle for 30 min before digital images of their dispersions were taken.

2.3.2 Zeta Potential

The change of surface charges of CNTs was investigated by zeta potential measurements at each stage of functionalisation. Samples were prepared by dispersing ~ 1 mg particles in 1.5 mL of 10 mM PBS and sonicated for 5 min at RT. The zeta potential for samples were measured using Zetasizer Nano ZS (Malvern Panalytical, UK), at RT, in triplicates and repeated for three independent batches. The average result was taken as the final zeta potential for each step.

2.3.3 Attenuated total reflection-Fourier transform infrared spectroscopy (ATR-FTIR)

The different functional groups expected on the surface of the carbon nanotubes were characterised by ART-FTIR at each reaction step. All samples were prepared by drying at 80^{o}C for at least 24 h until all the dispersion solvent had evaporated completely. Using Frontier^{TM} FTIR spectrometer (PerkinElmer, USA), each sample was analysed at RT in the spectral range of 4000-800 cm^{-1} with a total of 32 scans per run.

2.3.4 Transmission electronic microscope (TEM)

The successful coating of PDMAEMA brush on carbon nanotubes were morphologically characterised by TEM. Samples were prepared by dropping the diluted dispersions onto a 300-mesh carbon coated copper grid and air dried at RT, after which they were observed using a

Philips CM12 transmission electron microscope (FEI Electron Optics, Netherlands) with a Tungsten filament and a Veleta – 2k x 2k side-mounted TEM CCD Camera (Olympus, Japan). The TEM was operated at an accelerating voltage of 80 kV, the spot size was set at 2 and an objective aperture was used.

2.3.5 High resolution transmission electronic microscope (HRTEM)

HRTEM images were acquired on a FEI Tecnai G2 F20 microscope operated at 200 kV. Samples were prepared by dropping the diluted dispersions onto a 300-mesh lacey carbon coated copper grid and air-dried at RT. Prior to imaging, all the samples underwent a beam showering procedure of about 30 minutes under the electron beam to avoid contamination during subsequent imaging at high magnification.

2.3.6. Energy dispersive X-Ray spectroscopy (EDX)

EDX analyses on the samples were performed on a FEI Magellan 400L HRSEM coupled to an Oxford Instruments windowless Ultim Extreme EDX with 100 mm^2 sensor area, which is especially suitable to detect light elements. Experiments were carried out at 10 kV operating voltage to allow for the detection of all the elements present in the sample. Diluted dispersions of the samples were drop casted on Si wafer chips and left to dry in air. The composition values are the average of 3-5 measurements.

2.3.7. Thermogravimetric analysis (TGA)

The dry mass of functional groups synthesised on the carbon nanotubes was studied by TGA at each reaction step. All samples were prepared by drying at 80ºC for at least 24 h until all the dispersion solvent had evaporated completely. Using Q500 Thermogravimetric Analyzer (TA instruments, USA), under N_2 atmosphere, ~ 5 mg of the dried samples were analysed from RT to 1000ºC at a heating rate of 10ºC/min. Percentage weight losses were determined at 600ºC as previously reported [24] [25].

2.4 Nucleic acids loading on polymer brush coated carbon nanotubes

The effect of architectures of PDMAEMA brush-CNT hybrids on their interaction with nucleic acids (siRNA, ssDNA and plasmid) were assessed using gel electrophoresis. Nucleic acids (1 μg) were used to complex with each oCNT-PDMAEMA at different N/P ratios. The N/P ratio is the ratio of amine groups (N, nitrogen) on positively charged polymers to the phosphate groups (P) on the negatively charged nucleic acid. It is important to determine the N/P ratio of a cationic polymer-based nucleic acid complex as this character can influence many other properties such as the surface charge, size, and stability of the nucleic acid complex. The calculation of the N/P ratio is described as follows, and the units used are based on the international unit system. A 20−21 bp siRNA double strand contains 40−42 phosphate atoms. The total phosphate atoms can be calculated as n × P, where n is the total number of moles of siRNA used and P is the phosphate atoms per molecule. Nitrogen moles in the cationic polymer are calculated as M × V × N, where M is the molarity of the cationic polymer stock solution based on the repeat unit, V is the volume of the cationic polymer, and N is the number of nitrogen atoms in one monomer unit of the cationic polymer. Thus, the N/P ratio can be calculated as (M × V × N)/(n × P). After complexation, the corresponding gel loading dye purple or GelRed was added to each sample before loading to 2% agarose gel in sodium boric buffer (pH 8). The gel was run at 220 V for 10 min and subsequently imaged using ChemiDoc MP™ Imaging system (Bio-Rad Laboratories Inc., USA) and analysed using Image Lab™ software.

2.5 Cell viability

B16-F10 cell line (mouse melanoma cell line) was used for the *in vitro* studies. B16-F10 cells were cultured in RPMI-1640 medium supplied with 10% FCS, 1% pen-strep (Penicillin-Streptomycin) and 1% glutamine. The cell culture medium was changed every other day and cells were passaged before becoming confluent. In this study, a modified lactate dehydrogenase

(LDH) assay was applied to assess the cell viability of B16-F10 cells after incubation with different siRNA negative control complexes. Briefly, 50 k/well of B16-F10 cells were seeded in a 24 well plate one day prior the study. Subsequently, the medium was discarded and cells were washed with PBS once. OPTI-MEM serum free medium (400 μL) was added to each well. siRNA complexes (oCNT-DS/siRNA, oCNT-DSI+/siRNA or Lipo/siRNA, 100 μL for each complex) were prepared at N/P ratios of 0.5, 1, 2, 5 and 10 in OPTI-MEM serum free medium and added dropwise to B16-F10 cells with a final siRNA concentration of 50 nM and left to culture for 4 h before the medium was replaced with 500 μL complete culture medium for a further 48 h culturing. After 48 h, the medium was removed, and cells were washed with PBS once. Cells were then lysed with 500 μL of 1% Triton X-100 PBS solution for 1 h at 37°C. The plate was then centrifuged at 4,000 rpm for 30 min at RT. Supernatant (30 μL) was transferred to a new 96-well plate, followed by adding 30 μL of LDH reagent. The plate was incubated in dark for 20 min before adding 30 μL of stop solution. The bubbles were removed with a needle before reading the absorbance at 490 nm with a plate reader. The cell viability was calculated using the equation below.

$$\text{Cell viability \%} = \frac{A_{490}\,(\text{treated cells}) - A_{490}\,(\text{negative control})}{A_{490}(\text{untreated cells}) - A_{490}(\text{negative control})} \times 100 \qquad \text{Equation 1}$$

2.6 Cellular uptake

The cellular uptake study of different siRNA complexes was performed in B16-F10 cells. Here, a fluorescent Atto 655 siRNA was used to complex different carbon nanotube hybrids. These complexes (oCNT-DS/siRNA and oCNT-DSI+/siRNA) were prepared using the protocol described in cell viability study with N/P varied from 0.5 to 10 and a final siRNA concentration of 50 nM. Consequently, siRNA complexes were incubated with B16-F10 cells (50 k/well in 24 well plate) for 4 h in serum free OPTI-MEM medium and followed by replacing medium with full culture medium a further 48 h culturing. Free Atto siRNA (50 nM) was used as control and Lipofectamine 2000/Atto 655 siRNA was prepared according the product manual. After

48 h, cells were harvested and collected in polystyrene round bottom 12 x 75 mm^2 flow tubes. Cells were washed three times with PBS, centrifuged at 400 g for 5 min and resuspended in 200 μL of ice-cold PBS with 10% FCS,1% sodium azide. Cells were analysed with flow cytometry (BD FACSCalibur, using CellQuest software) using 640 nm excitation and a 670 nm bandpass filter, 10,000 events per sample are analysed. The fold increase of mean fluorescence intensity compared to untreated cells for each sample was used to express degree of cell uptake.

2.7 siPD-L1 transfection

PD-L1 is highly expressed on B16-F10 cells so they were chosen to test the transfection efficiency of the prepared hybrids. In this transfection assay, 100 k/well of B16-F10 cells were seeded in a 12 well plate 24 h prior study. oCNT-DS/siPD-L1 and oCNT-DSI+/siPD-L1 were prepared at N/P ratios of 2, 5, and 10 with a final siPD-L1 concentration of 50 nM. The medium was removed, and cells were washed with PBS once before adding 800 μL of OPTI-MEM serum free medium. 200 μL of siPD-L1 complex in OPTI-MEM serum free medium was added dropwise to the cells and left incubation for 4 h in cell culture incubator. Lipofectamine 2000/siPD-L1 was prepared according the product manual and used as a positive control. For control cells, 1 mL of serum free OPTI-MEM media was added. After 4 h, the medium was replaced with full culture medium and cultured for additional 48 h. B16-F10 cells were then harvested and collected in polystyrene round bottom 12 x 75 mm^2 flow tubes. Cells were washed with PBS and resuspended in 100 μL of PBS with 3% FCS, in which 50 μL of cell suspension was transferred to a new tube for isotype staining. Phycoerythrin (PE) anti-PD-L1 (or the corresponding isotype) with a concentration of 0.1 μg/mL was added to the cell suspension and left to incubate at RT for 20 min in dark. Cells were then washed three times with PBS, centrifuged at 400 g for 5 min and resuspended in 200 μL of ice-cold PBS with 10% FCS, 1% sodium azide. Cells were analysed with flow cytometry (10,000 events per sample)

using 488 nm excitation and a 585 nm bandpass filter. The knock-down efficiency of PD-L1 was calculated using the equation below.

$$\text{Knock down efficiency \%} = \left(1 - \frac{\text{MFI}_{\text{siRNA complex}} - \text{MFI}_{\text{siRNA complex isotype}}}{\text{MFI}_{\text{untreated cells}} - \text{MFI}_{\text{untreated cell isotype}}}\right) * 100 \qquad \text{Equation 2}$$

2.8 Statistics

Quantitative data were expressed as mean ± SD (standard deviation). Significant differences were examined using one-way ANOVA followed by Tukey's multiple comparison test.

3. Results and Discussions

3.1 Synthesis and characterisation of cationic polymer brush coated carbon nanotubes

Covalent grafting polymers onto CNTs has been extensively accomplished by the 'grafting-to' technique *via* esterification[26] or amidation[27] reactions in the past few decades. However, the loss in conformational entropy of the polymer significantly suppresses chains from diffusing to and reacting with CNTs, which leads to inefficient grafting. Growth of polymer chains using 'grafting-from' strategy is one of the best alternatives to produce dense polymer brushes on CNTs. However, anchoring the initiators on CNTs still remains one of the most challenging steps of synthesising polymer brushes *via* 'graft from' method due to the lack of chemical reactivity of CNTs. Several approaches have been developed to tackle this problem. Yan et al.[28-29] reported a typical initiator anchoring process from the CNTs, which involves the oxidation of CNTs, modification with thionyl chloride to form CNT-COCl, reacting with glycol to form CNT-OH and finally initiator coated CNTs were obtained by reacting with 2-bromo-2-methylpropionyl bromide. These functionalisation methods usually involve serious steps of complicated chemical reactions in harsh conditions, either with direct functionalisation of CNTs or pre-synthesis of initiators[30] that are specifically designed to suit the surface chemistry of functionalised CNTs. Additionally, the grafting density was limited and difficult

to control, as it depends on the availability of the functional groups on CNTs. It was reported that the end and sidewall were usually the most chemical reactive sites of CNTs.[31]

In this study, oxidation was applied to reduce the length of pCNTs, which is around several microns as presented with TEM images in Figure S1. Inspired by the adhesive behaviour of mussel proteins, biocompatible and uniform PDA coating can be formed on the surfaces of CNTs by spontaneous self-polymerisation of dopamine under mild alkaline conditions, which significantly alters the surface properties of CNTs, such as hydrophilicity, biofunctionality, dielectricity, mechanical properties *etc*.[22] The high concentration of catechol and amine groups on the PDA surface provide an opportunity for homogenously anchoring initiator molecules with high density on the surface of CNTs. Subsequently, SI-ATRP was employed for the controlled grafting of cationic PDMAEMA brushes from CNTs. Four types of brush grafted CNTs with precisely controlled polymer chain density and length, namely DL, DS, SL and SS brush coated CNTs were synthesised by varying the initiator concentration and controlling the polymerisation time. Dispersibility, zeta potential measurements, ATR-FTIR, TGA and TEM were applied collectively to monitor the progress of the modification and polymerisation.

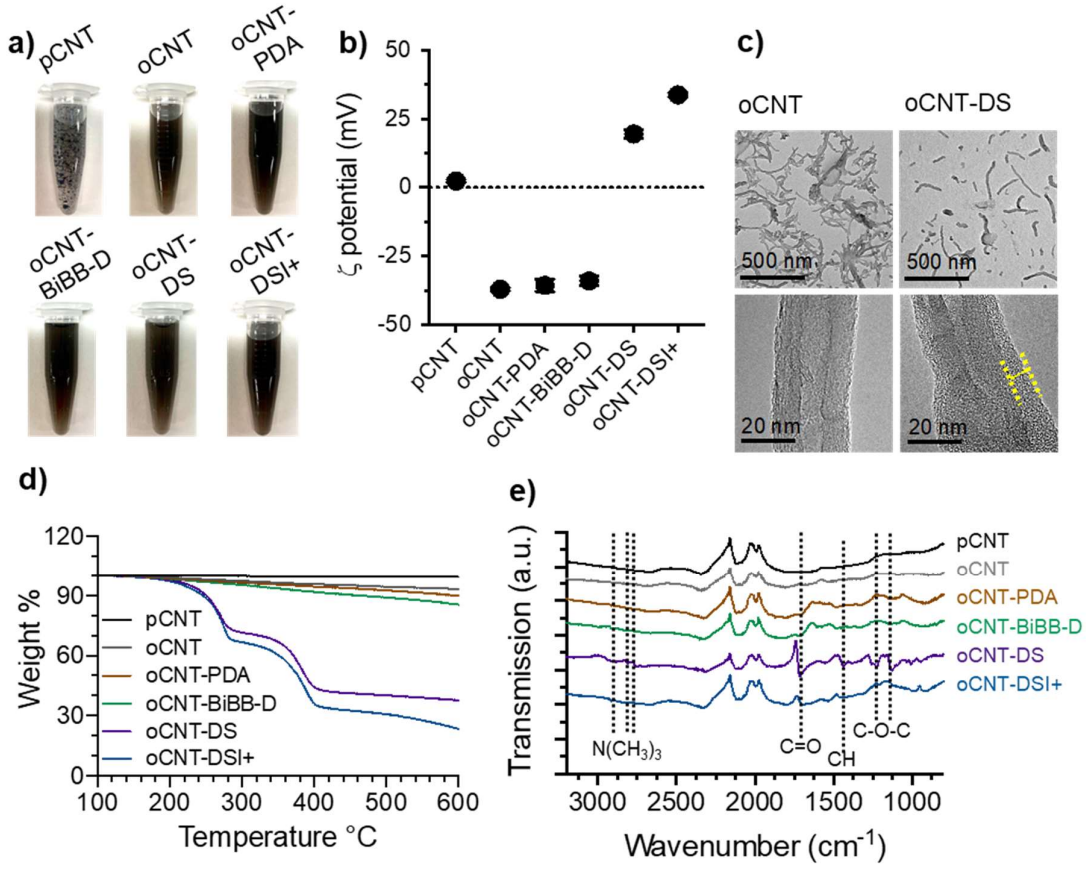

Figure 1. Characterisation of cationic polymer brush grafted carbon nanotubes. a) Dispersity in 1 X PBS. **b)** Zeta potential measured in 10 mM PBS, values are expressed as mean ± SD, where n=3. **c)** TEM (top two images with 500 nm scale bar) and HRTEM (bottom two images with 20 nm scale bar) of oCNT and oCNT-DS, highlighted area in HRTEM marks the polymer brush coatings. **d)** TGA of each reaction step measured from 100-600 ºC for the synthesis of DS brush coated carbon nanotube. **e)** FTIR of each reaction step with wavenumber range from 800-3200 cm^{-1} for the synthesis of DS brush coated carbon nanotube, with dash lines indicating the characteristic peaks after functionalisation.

3.1.1 Dispersion and zeta potential characterisation

Dispersion for CNTs at each stage of functionalisation in 1X PBS is dictated by their physicochemical properties. Figures 1a and S2 show that before any modification, pCNTs underwent sedimentation in PBS due to the highly hydrophobic surface properties and lack of functional groups, which was also indicated of their neutral zeta potential shown in Figure 1b. After oxidation, the dispersion of oCNT in PBS was improved as there was only slight

aggregation of nanotubes occurring after two hours. Together with the highly negative zeta potential measured for oCNT (-37.1 ± 0.6 mV), it showed successful oxidation of pCNTs, in which a large numbers of oxygen containing polar moieties including –COOH, -C=O and -OH were efficiently incorporated at the open ends and defect sites along the CNTs surface after treating with strong acids[32]. Zeta potentials after PDA coating or initiator deposition remained negative charge around -30 mV, which is attributed to the negatively charged -OH groups on oCNT-PDA and the bromo groups on oCNT-BiBB. As a result, dispersion of oCNT-PDA and oCNT-BiBB in PBS was better than oCNT, yielding a dark dispersion of homogenous colour with complete absence of aggregation for long term storage. After polymerisation, the charge on the carbon nanotube surface was reversed from highly negative to positive indicating successful grafting of the carbon nanotubes with a cationic PDMAEMA shell. There zeta potential for the SS brush type (13.6 ± 2.6 mV in Figure S3) was slightly lower than the other three brushes which all had a zeta potential of ~ 20 mV. In PBS (pH 7.4), the tertiary amines of pH sensitive PDMAEMA are only slightly positively charged, hence, the SS brush with a lower abundance of the cationic charges present was expected to have a lower zeta potential in comparison to the other brush types which was observed. All types of oCNT-PDMAEMA were easily suspended forming stable colloidal dispersions in PBS (Figure S2). After quaternisation, the zeta potential for each hybrid became highly positive (> 30 mV) owing to the permanent positive charge of the quaternary amines, regardless of the surrounding pH.

3.1.2 Morphology characterisation

Morphological changes before and after polymerisation were visualised through TEM and HRTEM. pCNTs have highly crystalline structure with low defects degree on its outer surface walls[33] displaying a tubular structure with neat, undamaged edges. TEM images also confirmed successful oxidation of pCNT, with obvious shortening of the tubes for oCNT (Figure 1c). After PDMAEMA brush growth, the thickness across the side walls of the nanotubes increased.

oCNT-DS (Figure 1c, highlighted dash lines) showed an obvious organic layer of polymer brush around the CNTs compared with oCNT under HRTEM, which indicated successful polymerisation. The organic layer was also visible for the other brush coated CNTs, namely oCNT-SS, oCNT-SL and oCNT-DL, as shown in Figure S4. The coating degree was observed to be higher for the dense brush coatings than for the sparse coated samples. The different modification steps were also followed by EDX spectroscopy (Figure S5). EDX analysis on oCNT sample showed carbon and oxygen peaks, as expected after the oxidation of the purified CNTs. Upon polymerisation, presence of N from the PDMAEMA structure became evident (see oCNT-DS spectra). Bromine peaks should also appear but overlap in energy with aluminium, which is an artefact of the measurement. After the quaternisation step, additional peaks corresponding to iodine became visible in oCNT-DSI+ spectra, proving the success of the quaternisation reaction. The analysis of light elements from EDX is semiquantitative as sometimes these elements could be resourced from the air and silicon wafer support. The atom percentages of C, N, and O of oCNT-DL, oCNT-DS, oCNT-SL, and oCNT-SS are shown in Table S1, where the N/C ratios related to the amount of the polymer brush on CNTsincreased in the following order: DL > DS > SL > SS. The same trend of increasing brush functionalization was observedby TGA.

3.1.3 TGA characterisation

TGA was employed to measure the degree of functionalisation and thermal stability of the CNTs at each synthesis step through characterisation of decomposition behaviour of the different samples. Pristine carbon nanotubes underwent minimal decomposition at temperatures up to 600ºC due to their high thermal stability[34] and any significant weight loss for CNTs observed prior to 500ºC is likely due to presence of impurities generated during its manufacture, which decompose at lower temperatures[35]. Figure 1d and S6 showed that the weight loss percentage of the CNTs increased with each successive functionalisation measured

at 600ºC. After polymerisation, a characteristic two-stage PDMAEMA decomposition was observed during the TGA study. The first degradation occurred in the range 210-280ºC, which was attributed to the elimination of side-chain groups of PDMAEMA. The second degradation stage was from 280-400ºC and was mainly attributed to the decomposition of carbon skeletons, especially in the central chain backbone. Expectedly, this behaviour was less evident with the TGA thermogram for sparse brush formation in Figure S6 compared to dense brush formation since the overall PDMAEMA amount grafted onto the carbon nanotubes was significantly lower. The overall decomposition percentage at each reaction step was summarised in Table S2 to quantify the amount of cationic polymer brush on CNTs.

3.1.4 FTIR characterisation

The chemical composition of the CNTs was studied through ATR-FTIR after each step of modification. Figure 1e and S7 showed that all CNTs displayed peaks in the region 1900-2300 cm^{-1} corresponding to the C-C bonds from the graphitic backbones. After oxidation, the spectra remained the same for oCNT probably because the degree of oxidation was not high enough for it to be detected. After PDA coating, new peaks at 1700 cm^{-1} (C=O stretching) and 1150 cm^{-1} (C-O stretching) appeared for oCNT-PDA due to the ester groups introduced. After ATRP initiator deposition, no obvious spectral change was detected for oCNT-BiBB-S compared to oCNT-PDA due to detectable chemical structure of the initiator is similar to that of the PDA coatings. It could also probably because of the ultrathin layer of the initiator to be detected within the sensitivity of the FTIR machine, as indicated by TGA showing the sparse initiator coating was only 0.5% (Table S2). However, the spectra for oCNT-BiBB-D showed slightly more intense peaks for C=O and C-O stretching indicative of the increase in surface ester moieties brought by dense initiator depositions. The peaks between 2770−2820 cm^{-1} were attributed to the $-N(CH_3)_3$ stretching vibrations, which are only found in spectra for PDMAEMA.[17] This further demonstrated successful polymerisation from the initiators for all

the oCNT-PDMAEMA hybrids. Other feature band at 1450 cm^{-1} corresponding to the -$N(CH_3)_3$ deformational stretching vibrations. In addition, there were more intense bands for C=O vibrations at 1700 cm^{-1} and for C-O-C at 1150 cm^{-1} compared to previous functionalisation steps indicting extra incorporation of ester groups from the PDMAEMA brushes. The intensities of the PDMAEMA feature bands amongst each brush type also varied with dense brush hybrids displayed higher frequencies of these characteristic bands compared to sparse brush hybrids. Finally, after quaternisation with methyl iodide, the quaternary ammonium salts in oCNT-PMETAI displayed weaker intensity of the characteristic PDMAEMA peaks, which were slightly shifted to higher wavenumbers.

3.2 Nucleic acids loading on polymer brush coated carbon nanotubes

PDMAEMA is a weak poly base since its DMAEMA monomeric units possess tertiary amines which are cationic depending on the surrounding pH.[36] At physiological conditions, PDMAEMA possesses a slightly positive charge which allows them to spontaneously associate with the anionic nucleic acids.[37] Dense crowding of cationic polymer brushes have been shown to provide unique environments for highly stable RNA uptake.[17] However, comprehensive investigation on how the architectures of brush modified CNTs affect the binding of different shapes and types of nucleic acids have not yet been studied. In this context, the binding of siRNA, ssDNA and plasmid DNA with the four types of brush-CNT hybrids were assessed. Figure 2 showed the gel electrophoresis study for siRNA binding onto the four types of oCNT-PDMAEMA materials tested at different N/P ratios of 1, 5 and 10. Free siRNA was used as control in each group. The images presented were the unbound siRNA, in which higher intensity of siRNA indicates less siRNA capture by the brush-CNT hybrids. Overall, the siRNA binding for each vector increased with increasing N/P ratios, demonstrating the highest siRNA loading capacity at N/P=10 due to more cationic polymers present.

oCNT-DS displayed the highest siRNA loading of the four brush types, which suggested the architecture of the brush plays a crucial role in binding with siRNA regardless of the amount of cationic polymers has been introduced. The polymerisation process can be ascertained from a linear first-order kinetic plot, accompanied by a linear increase in polymer molecular weights.[38] Therefore, when growing in the linear range, PDMAEMA could have formed densely grafted brush-like chain conformation, which provides a stronger entropic drive for the adsorption of anionic nucleic acids to stabilise the structure (Figure 2, oCNT-DS).[17, 19] The deactivation of the polymerisation was pronounced when the growth kinetics was not in a linear fashion,[39] typically occurred with long polymerisation time that only part of the polymer chains were able to extend. Consequently, a mushroom-like conformation could have formed on top of the brush-like structure (Figure 2, oCNT-DL), resulting in steric hindrance to allow further penetration of nucleic acids into the brush-like region compared to DS brush. When cationic polymer chains were initiated from a surface coated with sparse initiators, meaning the distance between two initiators sites was much longer than the polymer chain length,[20] the formation of lose and mushroom like morphology of polymer coatings occured[20, 40] on CNTs (oCNT-SS and oCNT- SL).

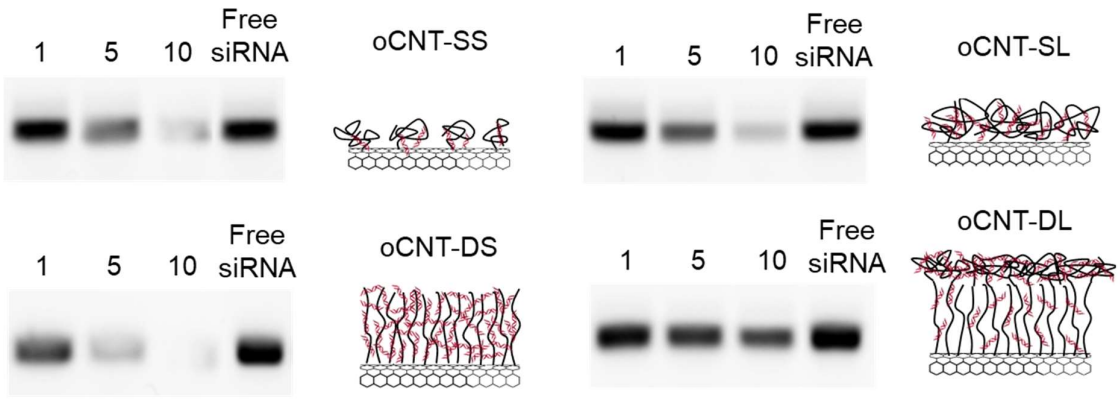

Figure 2. siRNA binding with different brush-CNT hybrids. Gel electrophoresis study of oCNT-SS, oCNT-SL, oCNT-DS and oCNT-DL complexed with 1 µg siRNA at N/P ratio of 1, 5 and 10 in 1 X PBS respectively . Free siRNA was used as control and the images presented were the unbound siRNA with higher intensity indicates less siRNA binding to the brush-CNT

hybrids; schematic illustrations were presented beside each gel image, indicating the different interaction mechanisms.

In this study, the adsorption of siRNA on the two types of sparse brushes exhibited similar trends, demonstrating minimal architectural impact of the polymers on siRNA binding. However, the amount of the sparse brush modified CNTs were enormously higher than dense brush coated CNTs as show in Table S3. Almost ten times of sparse brush CNT hybrids in weight was required to complex the same amount of nucleic acids as compared to dense brush CNTs. This could limit the further application of sparse brush modified CNTs for *in vitro* studies to meet the safe dosage of the CNTs hybrids whilst still maintain similar level of siRNA delivery efficiency.

Further gel electrophoresis studies were carried out for ssDNA(CpG) and plasmid (Figure S8a,b), which showed similar trend and correlated with the findings for siRNA adsorption on four different types of hybrids (Figure 2). Likewise, the DS brush exhibited the highest binding to both ssDNA and plasmid at all tested N/P ratios. This provides the evidence that DS brush modified CNTs could be applied to load various types of nucleic acids with different shapes, molecular weight, size, *etc*. more efficiently than its counterparts due to its unique architecture. To achieve more condensation with nucleic acids, higher N/P ratios to render the polyplexes with a net positive charge were usually introduced. However, excess cationic charge could possibly lead to more cytotoxicity, hence the delivery vector that achieves maximal loading at lower N/P ratio is more desirable. Therefore, oCNT-DSI+ were investigated for their siRNA loading as shown in Figure S8c. Owing to their highly permanent positive charge, these strong polyelectrolytes exhibited higher binding efficiencies compared with the non-quaternised brushes (Figure 2). Taken together, DS brush-CNT hybrids are of more interest for further *in vitro* studies.

3.3 Cell viability

The expansion of CNTs based materials for biomedical applications makes researchers more cautious regarding their safety issues.[41] In recent years, conflicting results have been reported that some have shown CNT induced morphological alterations of cellular structures[42], DNA damage[43] and cell apoptosis[44] *etc*., while others demonstrated CNTs do not induce apparent cytotoxicity[9, 45-46]. Numerous studies have underlined the relation between the biocompatibility of CNTs and their physicochemical properties and how the purity and surface modifications of CNTs have made huge impact to their cytotoxicity.[47-49] Meanwhile, different assays including 3-(4,5-dimethylthiazol-2-yl)-2,5-diphenyltetrazolium bromide) tetrazolium reduction (MTT)[50], lactate dehydrogenase (LDH)[48], flow cytometry-based Annexin V/PI (propidium iodide) staining[51], and other water soluble tetrazolium salt-based assays have been introduced to assess the cytotoxicity of CNTs, which may partially explain the variety in cell toxicity of CNT-based materials. We have previously reported the modified LDH assay [48] as a sensitive and reliable assay for the accurate assessment of cell viability of CNTs, which was used in this study.

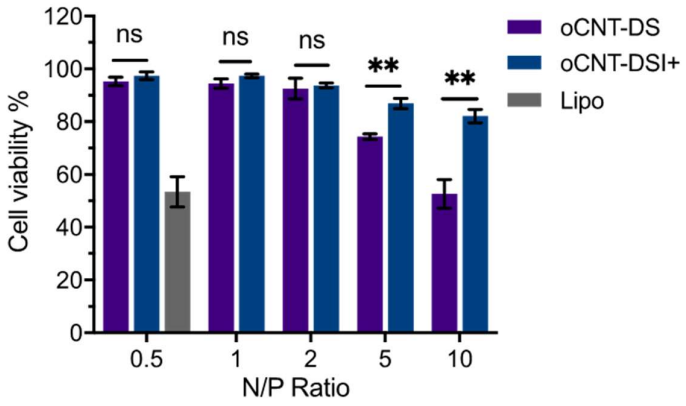

Figure 3. Viability test of B16-F10 cells treated with different siRNA complexes. Cell viability was tested with modified LDH assay. B16-F10 cells were treated with oCNT-DS/siRNA and oCNT-DSI+/siRNA complexes at different N/P ratios from 0.5 to 10 in OPTI-MEM serum free medium for 4 h, followed by replacing with full culture medium for further 48 h incubation. Values are expressed as mean ± SD, where n=3. Statistical analysis was done on oCNT-DS/siRNA and oCNT-DSI+/siRNA (ns: no significant difference, p**<0.01).

The viability of B16-F10 cells was measured by modified LDH assay after treatment with oCNT-DS/siRNA and oCNT-DSI+/siRNA complexes at a series of N/P ratios. Lipofectamine/siRNA complexes as controls were prepared according to manufacturer's instruction. As shown in Figure 3, lipofectamine/siRNA displays strong cytotoxicity with only 50 % of the cells survived after treatment. Both CNT based vectors showed a dose-dependent response on the cell viability that more cell deaths were exhibited with increasing N/P ratios. No obvious cytotoxicity was shown in both cases when N/P was below 5. Interestingly, oCNT-DS/siRNA displayed a significantly higher cytotoxicity compared with its quaternised form, oCNT-DSI+/siRNA, that the cell viability for oCNT-DS/siRNA was around 75% at N/P ratio of 5 and only 52% when N/P ratio increased to 10. However, oCNT-DSI+/siRNA exhibited above 80% of cell viability at the highest concentration despite the only difference being the type of amine groups for the two vectors.

Some studies have demonstrated cationic polymers drastically disrupt the cells above a certain concentration[52] which occurs only when the polycation has a certain hydrophobicity. The stronger the hydrophobicity of the cationic polymer is, the more cooperatively the cells are disrupted.[52] At pH of 7.4, PDMAEMA brush is only partially protonated[36-37], which may result in more pronounced hydrophobic interactions between polymer chains rather than the hydration with the polar surroundings. Conversely, after quaternisation, PMETAI brushes became highly positively charged and hydrated in physiological conditions, as reported in other studies[36], which have shown a reduction of the contact angle between the two types of brushes, meaning the PMETAI is more hydrophilic than PDMAEMA[53]. Therefore, it is evident in our study that the hydrophobicity of the polymer brush type dominates and contributes to the cytotoxicity rather than the positive charge density.

3.4 Cellular uptake

Efficient cellular uptake represents one of the major hurdles towards the therapeutic use of siRNAs.[54] To compare different brush-CNT hybrids with their ability to deliver siRNAs to B16-F10 cells, Atto 655-labeled siRNAs were complexed with both oCNT-DS and oCNT-DSI+ at a series of N/P ratios. Free siRNA and Lipofectamine/siRNA complex were also used. Cell-associated fluorescence was determined by flow cytometry and the mean fluorescence intensity (MFI) of the cells was used as a measure for the amount of internalised siRNA in Figure 4a. Free Atto siRNA exhibited negligible cellular uptake (Figure 4b) with no obvious histogram shift compared with untreated blank cells. The level of lipofectamine-assisted uptake was around 3.5 times higher than the free siRNA with histogram showing a broader shift compared to other groups. The uptake of oCNT-DS/siRNA and oCNT-DSI+/siRNA remains relatively low at N/P ratios below 5. At the highest N/P ratio, it showed 12 times and 9 times higher uptake than free siRNA for oCNT-DS/siRNA and oCNT-DSI+/siRNA, respectively, indicating the presence of more cationic polymers facilitates the uptake of siRNA complexes. The findings were also in agreement with the cell viability result considering the cell membrane disruption caused by oCNT-DS/siRNA may promote its cellular internalisation.

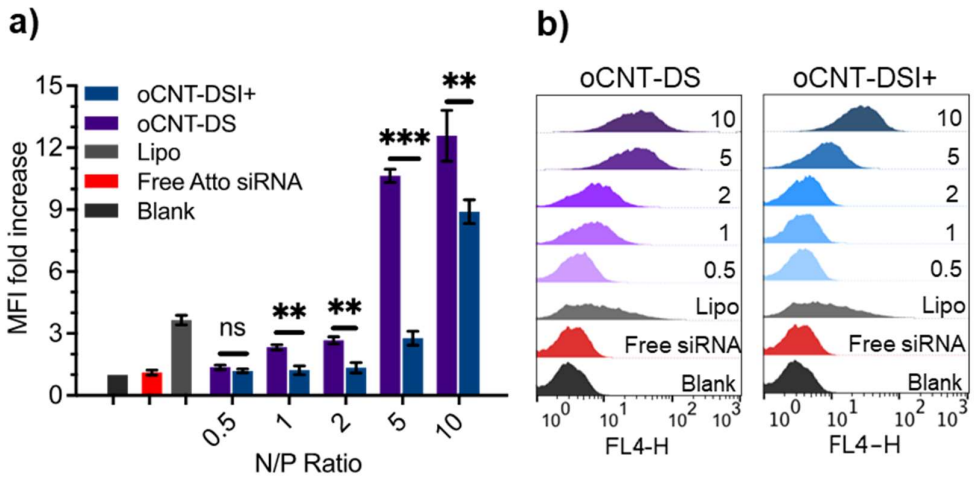

Figure 4. B16-F10 cellular uptake of atto 655 siRNA complexes. B16-F10 cells were treated with of oCNT-DS/atto 655 siRNA and oCNT-DSI+/atto 655 siRNA complexes at different N/P ratios from 0.5 to 10 in OPTI-MEM serum free medium for 4 h, followed by further 48 h incubation with full culture medium before analysis with flow cytometry. **a)** Mean fluorescence

intensity (MFI) fold increase as compared with blank cells, values are expressed as mean ± SD, where n=3. Statistical analysis was done on oCNT-DS/siRNA and oCNT-DSI+/siRNA (ns: no significant difference, p**<0.01, p***<0.001)**. b)** Histograms of the fluorescent intensity of the cells quantified by flow cytometry.

3.5 *In vitro* gene silencing

The high expression of checkpoint molecules such as PD-1 (programmed cell death protein 1) often causes immunosuppression.[55] Eliminating this resistance has emerged as a powerful approach to cancer therapy in recent years. Specifically, blocking PD-1 expressed on T cells or its receptors (PD-L1) expressed on antigen-presenting cells or tumour cells removes the immune suppression of nascent or dampened immune responses in the host. The use of siRNA to knockdown PD-L1 has been shown to be a promising strategy to sensitise cancer cells to T cell killing[56].

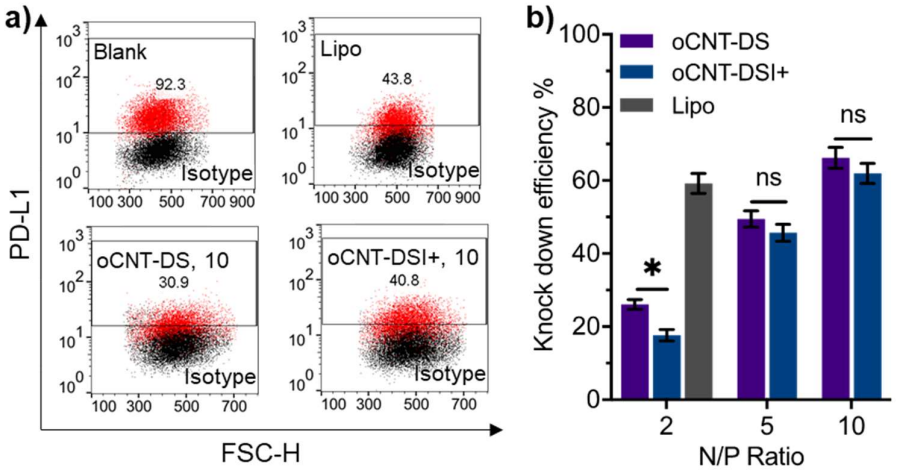

Figure 5. Knock down efficiency of PD-L1 for B16-F10 cells treated with siPD-L1 complexes. B16-F10 cells were transfected with oCNT-DS/siPD-L1 and oCNT-DS/siPD-L1 complexes at N/P=2, 5 and 10. Lipofectamine 2000 (Lipo)/siPD-L1 was used as a positive control according to manufacturer's instruction. Cells were incubated with siRNA complexes in OPTI-MEM serum free medium for 4 h, followed by replacing with full culture medium for further 48 h incubation. **a)** Dot blots of representative figures by flow cytometry with red showing the expression of PD-L1 and black representing the corresponding isotype for the same sample. **b)** Knock down efficiency quantified according the mean fluorescent intensity of each sample using Equation 2, values are expressed as mean ± SD, where n=3. Statistical

analysis was done on oCNT-DS/siRNA and oCNT-DSI+/siRNA (ns: no significant difference, $p * < 0.05$).

Given the high siRNA adsorption of DS brush modified CNT, the knockdown efficiencies of PD-L1 on B16-F10 cells with oCNT-DS/siPD-L1 and oCNT-DSI+/siPD-L1 were assessed. Lipofectamine/siPD-L1 was used as the positive control. Post transfection, B16-F10 cells were harvested and stained with PE anti-PD-L1 antibodies and the corresponding isotype, then analysed with flow cytometry. Representative dot plots for blank cells, Lipofectamine transfected cells and brush-CNT hybrids transfected cells were shown in Figure 5a and Figure S9. The MFI of the cells was used to calculate the knock down efficiencies of different siRNA carriers according to Equation 1 and showed in Figure 5b. B16-F10 cells exhibited a high expression of PD-L1 on the cell surface with above 90% of cells population showed PD-L1 positive. After transfection, an evident reduction of PD-L1 expression presented on lipofectamine group with around 60% of knock down efficiency. With increasing N/P ratios of siPD-L1 complexes of both brush-CNT hybrids, the enhancement in silencing activities was observed with 66 ± 5% and 62 ± 5% of knockdown efficiencies at the highest N/P ratios for oCNT-DS/siPD-L1 and oCNT-DSI+/siPD-L1 respectively, of which, oCNT-DS groups is significantly higher than Lipofectamine. This result demonstrated the capability of the brush coated vectors on efficient delivery of siPD-L1 to B16-F10 cells. No significant difference was observed between oCNT-DS/siPD-L1 and oCNT-DSI+/siPD-L1 groups although the uptake level of PDMAEMA brush coated CNTs is slightly higher than its quaternised form. This may be attributed to membrane disruption discussed in cell viability section and the mechanism of siRNA silencing that a low dose of siRNA was typically required to have effective silencing. However, in many cases, the actual siRNA amount that released in cytosol and incorporated to RNAi machinery was unclear. Conclusively, dense cationic polymer brush functionalised

CNTs demonstrated their potential as siRNA carriers to achieve efficient silencing of PD-L1 on B16-F10 cells.

Conclusion

By employing the mussel-inspired polydopamine chemistry and SI-ATRP, the synthesis of cationic polymer brush grafted CNTs was achieved with control over the coating chemistry and architecture. We concluded that DS cationic polymer brush coatings are superior in efficiently binding different nucleic acids compared to other architectures. DS brush coated CNTs also demonstrated higher levels of cellular uptake and transfection efficiency compared to commercially available agent. This novel cationic polymer brush grafted CNTs offers new capabilities for the rational design of delivery systems for genetic materials and potentially other combinatory approaches.

Acknowledgement

Danyang Li is a Maplethorpe Fellow. This project has received funding from the Maplethorpe Foundation, University of London. This project has received funding from the Brain Tumour Charity (GN-000398) and Institutional Link- British Council (IL4337313). We thank Dr Lim Yau for providing technical support of gel electrophoresis. ICN2 acknowledges financial support from the Spanish Ministry of Economy and Competitiveness, through the "Severo Ochoa" Programme for Centres of Excellence in R&D (SEV-2017-0706). BB acknowledges funding from Generalitat de Catalunya 2017 SGR 327.

References

(1) Huang, S. L. Liposomes in ultrasonic drug and gene delivery. *Adv Drug Deliv Rev* **2008,** *60*, 1167-76.
(2) Gao, X.; Huang, L. Cationic liposome-mediated gene transfer. *Gene Ther* **1995,** *2*, 710-22.

(3) Kim, Y. I.; Chung, J. W.; Park, J. H.; Han, J. K.; Hong, J. W.; Chung, H. Intraarterial gene delivery in rabbit hepatic tumors: transfection with nonviral vector by using iodized oil emulsion. *Radiology* **2006,** *240*, 771-7.
(4) Nishiyama, N.; Kataoka, K. Current state, achievements, and future prospects of polymeric micelles as nanocarriers for drug and gene delivery. *Pharmacology & Therapeutics* **2006,** *112*, 630-648.
(5) Ravi Kumar, M.; Hellermann, G.; Lockey, R. F.; Mohapatra, S. S. Nanoparticle-mediated gene delivery: state of the art. *Expert Opin Biol Ther* **2004,** *4*, 1213-24.
(6) Herrero, M. A.; Toma, F. M.; Al-Jamal, K. T.; Kostarelos, K.; Bianco, A.; Da Ros, T.; Bano, F.; Casalis, L.; Scoles, G.; Prato, M. Synthesis and characterization of a carbon nanotube-dendron series for efficient siRNA delivery. *J Am Chem Soc* **2009,** *131*, 9843-8.
(7) Nunes, A.; Amsharov, N.; Guo, C.; Van den Bossche, J.; Santhosh, P.; Karachalios, T. K.; Nitodas, S. F.; Burghard, M.; Kostarelos, K.; Al-Jamal, K. T. Hybrid polymer-grafted multiwalled carbon nanotubes for in vitro gene delivery. *Small* **2010,** *6*, 2281-91.
(8) Karimi, M.; Solati, N.; Ghasemi, A.; Estiar, M. A.; Hashemkhani, M.; Kiani, P.; Mohamed, E.; Saeidi, A.; Taheri, M.; Avci, P.; Aref, A. R.; Amiri, M.; Baniasadi, F.; Hamblin, M. R. Carbon nanotubes part II: a remarkable carrier for drug and gene delivery. *Expert Opinion on Drug Delivery* **2015,** *12*, 1089-1105.
(9) Pantarotto, D.; Singh, R.; McCarthy, D.; Erhardt, M.; Briand, J. P.; Prato, M.; Kostarelos, K.; Bianco, A. Functionalized carbon nanotubes for plasmid DNA gene delivery. *Angew Chem Int Ed Engl* **2004,** *43*, 5242-6.
(10) Singh, R.; Pantarotto, D.; McCarthy, D.; Chaloin, O.; Hoebeke, J.; Partidos, C. D.; Briand, J. P.; Prato, M.; Bianco, A.; Kostarelos, K. Binding and condensation of plasmid DNA onto functionalized carbon nanotubes: toward the construction of nanotube-based gene delivery vectors. *J Am Chem Soc* **2005,** *127*, 4388-96.
(11) Battigelli, A.; Wang, J. T.; Russier, J.; Da Ros, T.; Kostarelos, K.; Al-Jamal, K. T.; Prato, M.; Bianco, A. Ammonium and guanidinium dendron-carbon nanotubes by amidation and click chemistry and their use for siRNA delivery. *Small* **2013,** *9*, 3610-9.
(12) Liu, M.; Chen, B.; Xue, Y.; Huang, J.; Zhang, L.; Huang, S.; Li, Q.; Zhang, Z. Polyamidoamine-grafted multiwalled carbon nanotubes for gene delivery: synthesis, transfection and intracellular trafficking. *Bioconjug Chem* **2011,** *22*, 2237-43.
(13) Liu, Z.; Winters, M.; Holodniy, M.; Dai, H. siRNA Delivery into Human T Cells and Primary Cells with Carbon-Nanotube Transporters. *Angewandte Chemie International Edition* **2007,** *46*, 2023-2027.
(14) Kam, N. W.; Liu, Z.; Dai, H. Functionalization of carbon nanotubes via cleavable disulfide bonds for efficient intracellular delivery of siRNA and potent gene silencing. *J Am Chem Soc* **2005,** *127*, 12492-3.
(15) Huang, Y. P.; Lin, I. J.; Chen, C. C.; Hsu, Y. C.; Chang, C. C.; Lee, M. J. Delivery of small interfering RNAs in human cervical cancer cells by polyethylenimine-functionalized carbon nanotubes. *Nanoscale Res Lett* **2013,** *8*, 267.
(16) Krishnamoorthy, M.; Li, D.; Sharili, A. S.; Gulin-Sarfraz, T.; Rosenholm, J. M.; Gautrot, J. E. Solution Conformation of Polymer Brushes Determines Their Interactions with DNA and Transfection Efficiency. *Biomacromolecules* **2017,** *18*, 4121-4132.
(17) Li, D.; Sharili, A. S.; Connelly, J.; Gautrot, J. E. Highly Stable RNA Capture by Dense Cationic Polymer Brushes for the Design of Cytocompatible, Serum-Stable SiRNA Delivery Vectors. *Biomacromolecules* **2018,** *19*, 606-615.
(18) Li, D.; Wu, L.; Qu, F.; Ribadeneyra, M. C.; Tu, G.; Gautrot, J. Core-independent approach for polymer brush-functionalised nanomaterials with a fluorescent tag for RNA delivery. *Chem Commun (Camb)* **2019,** *55*, 14166-14169.

(19) Qu, F.; Li, D.; Ma, X.; Chen, F.; Gautrot, J. E. A Kinetic Model of Oligonucleotide-Brush Interactions for the Rational Design of Gene Delivery Vectors. *Biomacromolecules* **2019,** *20*, 2218-2229.
(20) Barbey, R.; Lavanant, L.; Paripovic, D.; Schuwer, N.; Sugnaux, C.; Tugulu, S.; Klok, H. A. Polymer brushes via surface-initiated controlled radical polymerization: synthesis, characterization, properties, and applications. *Chem Rev* **2009,** *109*, 5437-527.
(21) Thi Mai Hoa, L. Characterization of multi-walled carbon nanotubes functionalized by a mixture of HNO3/H2SO4. *Diamond and Related Materials* **2018,** *89*, 43-51.
(22) Song, Y.; Ye, G.; Lu, Y.; Chen, J.; Wang, J.; Matyjaszewski, K. Surface-Initiated ARGET ATRP of Poly(Glycidyl Methacrylate) from Carbon Nanotubes via Bioinspired Catechol Chemistry for Efficient Adsorption of Uranium Ions. *ACS Macro Letters* **2016,** *5*, 382-386.
(23) Hu, H.; Yu, B.; Ye, Q.; Gu, Y.; Zhou, F. Modification of carbon nanotubes with a nanothin polydopamine layer and polydimethylamino-ethyl methacrylate brushes. *Carbon* **2010,** *48*, 2347-2353.
(24) Hassan, H. A. F. M.; Smyth, L.; Rubio, N.; Ratnasothy, K.; Wang, J. T. W.; Bansal, S. S.; Summers, H. D.; Diebold, S. S.; Lombardi, G.; Al-Jamal, K. T. Carbon nanotubes' surface chemistry determines their potency as vaccine nanocarriers in vitro and in vivo. *Journal of Controlled Release* **2016,** *225*, 205-216.
(25) Hassan, H. A. F. M.; Smyth, L.; Wang, J. T. W.; Costa, P. M.; Ratnasothy, K.; Diebold, S. S.; Lombardi, G.; Al-Jamal, K. T. Dual stimulation of antigen presenting cells using carbon nanotube-based vaccine delivery system for cancer immunotherapy. *Biomaterials* **2016,** *104*, 310-322.
(26) Fernandez d'Arlas, B.; Goyanes, S.; Rubiolo, G. H.; Mondragon, I.; Corcuera, M. A.; Eceiza, A. Surface modification of multiwalled carbon nanotubes via esterification using a biodegradable polyol. *J Nanosci Nanotechnol* **2009,** *9*, 6064-71.
(27) Al-Jamal, K. T.; Gherardini, L.; Bardi, G.; Nunes, A.; Guo, C.; Bussy, C.; Herrero, M. A.; Bianco, A.; Prato, M.; Kostarelos, K.; Pizzorusso, T. Functional motor recovery from brain ischemic insult by carbon nanotube-mediated siRNA silencing. *Proc Natl Acad Sci U S A* **2011,** *108*, 10952-7.
(28) Kong, H.; Gao, C.; Yan, D. Controlled functionalization of multiwalled carbon nanotubes by in situ atom transfer radical polymerization. *J Am Chem Soc* **2004,** *126*, 412-3.
(29) Kong, H.; Gao, C.; Yan, D. Functionalization of Multiwalled Carbon Nanotubes by Atom Transfer Radical Polymerization and Defunctionalization of the Products. *Macromolecules* **2004,** *37*, 4022-4030.
(30) Qin, S.; Qin, D.; Ford, W. T.; Resasco, D. E.; Herrera, J. E. Polymer Brushes on Single-Walled Carbon Nanotubes by Atom Transfer Radical Polymerization of n-Butyl Methacrylate. *Journal of the American Chemical Society* **2004,** *126*, 170-176.
(31) Liu, P. Modifications of carbon nanotubes with polymers. *European Polymer Journal* **2005,** *41*, 2693-2703.
(32) Hu, H.; Yu, A.; Kim, E.; Zhao, B.; Itkis, M. E.; Bekyarova, E.; Haddon, R. C. Influence of the zeta potential on the dispersability and purification of single-walled carbon nanotubes. *J Phys Chem B* **2005,** *109*, 11520-4.
(33) Gómez, S.; Rendtorff, N. M.; Aglietti, E. F.; Sakka, Y.; Suárez, G. Surface modification of multiwall carbon nanotubes by sulfonitric treatment. *Applied Surface Science* **2016,** *379*, 264-269.
(34) Dlamini, N.; Mukaya, H. E.; Van Zyl, R. L.; Chen, C. T.; Zeevaart, R. J.; Mbianda, X. Y. Synthesis, characterization, kinetic drug release and anticancer activity of bisphosphonates multi-walled carbon nanotube conjugates. *Mater Sci Eng C Mater Biol Appl* **2019,** *104*, 109967.
(35) Datsyuk, V.; Kalyva, M.; Papagelis, K.; Parthenios, J.; Tasis, D.; Siokou, A.; Kallitsis, I.; Galiotis, C. Chemical oxidation of multiwalled carbon nanotubes. *Carbon* **2008,** *46*, 833-840.

(36) Santos, D. E. S.; Li, D.; Ramstedt, M.; Gautrot, J. E.; Soares, T. A. Conformational Dynamics and Responsiveness of Weak and Strong Polyelectrolyte Brushes: Atomistic Simulations of Poly(dimethyl aminoethyl methacrylate) and Poly(2-(methacryloyloxy)ethyl trimethylammonium chloride). *Langmuir* **2019,** *35*, 5037-5049.
(37) Agarwal, S.; Zhang, Y.; Maji, S.; Greiner, A. PDMAEMA based gene delivery materials. *Materials Today* **2012,** *15*, 388-393.
(38) Tsarevsky, N. V.; Pintauer, T.; Matyjaszewski, K. Deactivation Efficiency and Degree of Control over Polymerization in ATRP in Protic Solvents. *Macromolecules* **2004,** *37*, 9768-9778.
(39) Polanowski, P.; Hałagan, K.; Pietrasik, J.; Jeszka, J. K.; Matyjaszewski, K. Growth of polymer brushes by "grafting from" via ATRP – Monte Carlo simulations. *Polymer* **2017,** *130*, 267-279.
(40) Moh, L. C.; Losego, M. D.; Braun, P. V. Solvent quality effects on scaling behavior of poly(methyl methacrylate) brushes in the moderate- and high-density regimes. *Langmuir* **2011,** *27*, 3698-702.
(41) Kobayashi, N.; Izumi, H.; Morimoto, Y. Review of toxicity studies of carbon nanotubes. *J Occup Health* **2017,** *59*, 394-407.
(42) Shvedova, A.; Castranova, V.; Kisin, E.; Schwegler-Berry, D.; Murray, A.; Gandelsman, V.; Maynard, A.; Baron, P. Exposure to Carbon Nanotube Material: Assessment of Nanotube Cytotoxicity using Human Keratinocyte Cells. *Journal of Toxicology and Environmental Health, Part A* **2003,** *66*, 1909-1926.
(43) Zhu, L.; Chang, D. W.; Dai, L.; Hong, Y. DNA damage induced by multiwalled carbon nanotubes in mouse embryonic stem cells. *Nano Lett* **2007,** *7*, 3592-7.
(44) Bottini, M.; Bruckner, S.; Nika, K.; Bottini, N.; Bellucci, S.; Magrini, A.; Bergamaschi, A.; Mustelin, T. Multi-walled carbon nanotubes induce T lymphocyte apoptosis. *Toxicol Lett* **2006,** *160*, 121-6.
(45) Cherukuri, P.; Bachilo, S. M.; Litovsky, S. H.; Weisman, R. B. Near-infrared fluorescence microscopy of single-walled carbon nanotubes in phagocytic cells. *J Am Chem Soc* **2004,** *126*, 15638-9.
(46) Shi Kam, N. W.; Jessop, T. C.; Wender, P. A.; Dai, H. Nanotube molecular transporters: internalization of carbon nanotube-protein conjugates into Mammalian cells. *J Am Chem Soc* **2004,** *126*, 6850-1.
(47) Vittorio, O.; Raffa, V.; Cuschieri, A. Influence of purity and surface oxidation on cytotoxicity of multiwalled carbon nanotubes with human neuroblastoma cells. *Nanomedicine* **2009,** *5*, 424-31.
(48) Ali-Boucetta, H.; Al-Jamal, K. T.; Muller, K. H.; Li, S.; Porter, A. E.; Eddaoudi, A.; Prato, M.; Bianco, A.; Kostarelos, K. Cellular uptake and cytotoxic impact of chemically functionalized and polymer-coated carbon nanotubes. *Small* **2011,** *7*, 3230-8.
(49) Singh, P.; Samorì, C.; Toma, F. M.; Bussy, C.; Nunes, A.; Al-Jamal, K. T.; Ménard-Moyon, C.; Prato, M.; Kostarelos, K.; Bianco, A. Polyamine functionalized carbon nanotubes: synthesis, characterization, cytotoxicity and siRNA binding. *Journal of Materials Chemistry* **2011,** *21*, 4850-4860.
(50) Magrez, A.; Kasas, S.; Salicio, V.; Pasquier, N.; Seo, J. W.; Celio, M.; Catsicas, S.; Schwaller, B.; Forró, L. Cellular Toxicity of Carbon-Based Nanomaterials. *Nano Letters* **2006,** *6*, 1121-1125.
(51) Al-Jamal, K. T.; Kostarelos, K. Assessment of Cellular Uptake and Cytotoxicity of Carbon Nanotubes Using Flow Cytometry. In *Carbon Nanotubes: Methods and Protocols*; Balasubramanian, K.; Burghard, M., Eds.; Humana Press: Totowa, NJ, 2010; pp 123-134.

(52) Narita, T.; Ohtakeyama, R.; Matsukata, M.; Gong, J. P.; Osada, Y. Kinetic study of cell disruption by ionic polymers with varied charge density. *Colloid and Polymer Science* **2001,** *279*, 178-183.
(53) Zhu, L.-J.; Zhu, L.-P.; Zhao, Y.-F.; Zhu, B.-K.; Xu, Y.-Y. Anti-fouling and anti-bacterial polyethersulfone membranes quaternized from the additive of poly(2-dimethylamino ethyl methacrylate) grafted SiO2 nanoparticles. *Journal of Materials Chemistry A* **2014,** *2*, 15566-15574.
(54) Mescalchin, A.; Detzer, A.; Wecke, M.; Overhoff, M.; Wünsche, W.; Sczakiel, G. Cellular uptake and intracellular release are major obstacles to the therapeutic application of siRNA: novel options by phosphorothioate-stimulated delivery. *Expert Opinion on Biological Therapy* **2007,** *7*, 1531-1538.
(55) Perica, K.; Varela, J. C.; Oelke, M.; Schneck, J. Adoptive T cell immunotherapy for cancer. *Rambam Maimonides Med J* **2015,** *6*, e0004.
(56) Kwak, G.; Kim, D.; Nam, G.-h.; Wang, S. Y.; Kim, I.-S.; Kim, S. H.; Kwon, I.-C.; Yeo, Y. Programmed Cell Death Protein Ligand-1 Silencing with Polyethylenimine–Dermatan Sulfate Complex for Dual Inhibition of Melanoma Growth. *ACS Nano* **2017,** *11*, 10135-10146.